ACS OMEGA

http://pubs.acs.org/journal/acsodf

Article

Improved Skin Permeability after Topical Treatment with Serine Protease: Probing the Penetration of Rapamycin by Scanning Transmission X-ray Microscopy

Gregor Germer, Takuji Ohigashi, Hayato Yuzawa, Nobuhiro Kosugi, Roman Flesch, Fiorenza Rancan, Annika Vogt, and Eckart Rühl*

Cite This: *ACS Omega* 2021, 6, 12213−12222

Read Online

ACCESS | Metrics & More | Article Recommendations | Supporting Information

ABSTRACT: Drug penetration in human skin ex vivo following a modification of skin barrier permeability is systematically investigated by scanning transmission X-ray microscopy. Element-selective excitation is used in the O 1s regime for probing quantitatively the penetration of topically applied rapamycin in different formulations with a spatial resolution reaching <75 nm. The data were analyzed by a comparison of two methods: (i) two-photon energies employing the Beer−Lambert law and (ii) a singular value decomposition approach making use of the full spectral information in each pixel of the X-ray micrographs. The latter approach yields local drug concentrations more reliably and sensitively probed than the former. The present results from both approaches indicate that rapamycin is not observed within the stratum corneum of nontreated skin ex vivo, providing evidence for the observation that this high-molecular-weight drug inefficiently penetrates intact skin. However, rapamycin is observed to penetrate more efficiently the stratum corneum when modifications of the skin barrier are induced by the topical pretreatment with the serine protease trypsin for variable time periods ranging from 2 to 16 h. After the longest exposure time to serine protease, the drug is even found in the viable epidermis. High-resolution micrographs indicate that the lipophilic drug preferably associates with corneocytes, while signals found in the intercellular lipid compartment were less pronounced. This result is discussed in comparison to previous work obtained from low-molecular-weight lipophilic drugs as well as polymer nanocarriers, which were found to penetrate the intact stratum corneum exclusively via the lipid layers between the corneocytes. Also, the role of the tight junction barrier in the stratum granulosum is briefly discussed with respect to modifications of the skin barrier induced by enhanced serine protease activity, a phenomenon of clinical relevance in a range of inflammatory skin disorders.

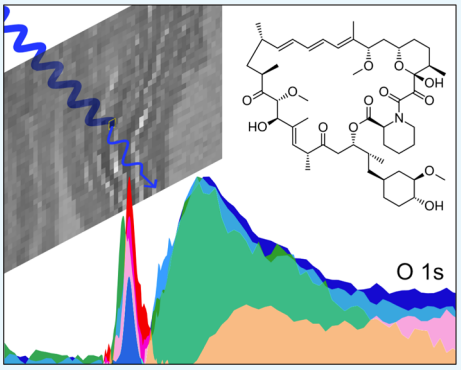

INTRODUCTION

Topical drug delivery is an attractive way for administering drugs dermally or transdermally, where the skin penetration properties depend strongly on the physicochemical properties of the drug and the formulation.[1] The skin represents for most drugs a barrier that has been investigated in detail by several aspects, which include barrier disruption methods.[2] The stratum corneum (SC), the top horny layer of skin, plays a key role in the barrier function of this organ.[3] Of specific interest are barrier disruptions caused by inflammatory skin diseases, such as atopic dermatitis and psoriasis.[4,5] Several drugs have been used for the topical treatment of these diseases, which include immunosuppressive macrolides, such as cyclosporin A and tacrolimus. However, according to the 500 Da rule for skin penetration, high-molecular-weight drugs have a limited skin penetration.[6] Therefore, new formulations have been developed to facilitate the dermal penetration of such drugs.[7]

Rapamycin (sirolimus) $C_{51}H_{79}NO_{13}$ (cf. inset of Figure 1) is an FDA-approved macrocyclic lactone with anti-proliferative properties used in cancer or immunosuppressive treatments, for example, after organ transplantation.[8] Related drugs, such as everolimus, have been used for successful cancer therapy.[9] Of specific interest is the topical application of rapamycin for the treatment of facial angiofibromas,[10,11] partially in combination with other drugs, such as calcitriol.[12] Short-term efficacy and safety aspects of rapamycin gels for patients with tuberous sclerosis complex have been investigated more recently.[13] Furthermore, human skin explants treated with rapamycin were investigated in a culture medium revealing histological changes and reduced keratinocyte proliferation.[8] Rapamycin is known to act as a mammalian target of

Received: February 26, 2021
Accepted: April 7, 2021
Published: April 28, 2021

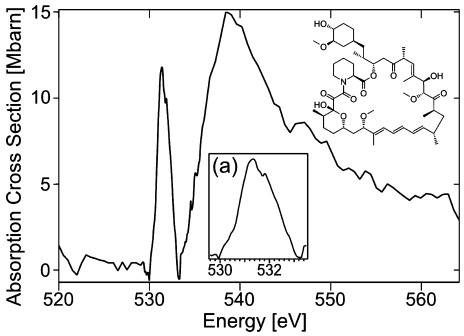

Figure 1. X-ray absorption cross section of rapamycin in the O 1s regime. The inset (a) shows the O 1s → π^* transition in greater detail. The structure of rapamycin is shown in the top right corner.

rapamycin (mTOR) inhibitor,[14−16] where the complexity of the mTOR pathway has been reviewed before.[17] Early work was concerned with cellular transport and uptake studies of this active substance, where the crucial parameters, such as temperature and dose, were identified.[18] Later work focused on the role of rapamycin on immune cells.[19] Of specific interest has been the formulation of rapamycin for topical use, where hydrophilic gels, ethanolic solutions, ointments, creams, and formulations in petrolatum have been used.[10,11] Dermal penetration enhancers, such as ethanol,[20] have also been used for the preparation of rapamycin formulations, where the long-term stability of such formulations has been evaluated as well.[11]

The detection of topically applied drugs penetrated in the different skin layers requires a method to probe low, ideally therapeutically relevant, concentrations. Spectroscopic studies need to be supplemented by microscopy approaches since the drugs are inhomogeneously distributed in the biological matrix, requiring the use of spectromicroscopy techniques. Multiple combinations of such techniques have been developed in the past and applied to biological matter. Often used are fluorescence labels due to their specific response and high sensitivity reaching single-molecule or -particle detection.[21] Furthermore, super-resolution techniques below the diffraction limit also increase significantly the detailed understanding of processes occurring in biological matter.[22] However, in the field of drug delivery, it appears to be advantageous to avoid labeling of drugs due to possible changes in their efficacy and transport properties. This requires the use of label-free detection schemes that have been developed over the last decades. Such methods directly probe drugs or molecular species of interest in the biological environment, including human skin ex vivo.[23] This is accomplished by exploiting their unique molecular properties. For example, absorption in the soft X-ray regime has been used in the past to probe with high-sensitivity drugs in human skin explants or other biological objects by scanning transmission X-ray microscopy (STXM).[24−28] Alternatively, Raman-based techniques have been used,[29−31] as well as atomic force microscopy (AFM)-based approaches.[32,33] Furthermore, mass spectrometry-based approaches have also been used.[23,34]

This work aimed at investigating the skin penetration of rapamycin in the skin with an intact or altered skin barrier. This hydrophobic (log P = 4.3)[35] and high-molecular-weight (M = 914.187 g/mol)[35] drug does not efficiently penetrate the skin barrier if topically applied, as predicted by the 500 Da rule.[6,36,37] Nevertheless, penetration of rapamycin might be enhanced by the serine protease trypsin. Trypsin applied in moderate concentrations capable of triggering inflammatory processes has been used as a stimulus in cell cultures to mimic enhanced serine protease activity, typically found in inflammatory skin diseases, such as atopic dermatitis.[38,39] It is also known that trypsin-like serine proteases in the SC are associated with desquamation.[40] These proteases are found to be more active in the outer SC than in the inner part of this skin layer. Earlier studies on the proteolytic activity in the SC indicate a linear temporal behavior in the range below 200 min.[41] Furthermore, the epidermal barrier function of the skin is known to depend on the serine protease CAP1/Prss8 in mice, disturbing the lipid composition of the SC, the corneocyte morphogenesis, and the processing of profilaggrin.[42] In humans, it is known that abnormal activity of serine proteases leads to a loss in barrier function, such as in ichthyosis. Furthermore, patients suffering from the Netherton syndrome are known to have an increased serine protease activity, leading to changes in barrier function, which is accompanied by an altered SC lipid composition with a preference for shorter chains and increased disorder of the lipids.[43,44] Recent work also highlights the increased drug penetration in serine protease pretreated ex vivo skin models with respect to the penetration of dexamethasone-loaded core-multishell nanocarriers.[39]

EXPERIMENTAL SECTION

The ex vivo human skin samples from abdominal skin and breast were obtained from different donors, who had agreed prior to donation. The study has been run in accordance with the Declaration of Helsinki guidelines and was approved by the Ethics Committee of Charité—Universitätsmedizin Berlin (Germany) (approval EA1/135/06, renewed in January 2019). Skin was used within a few hours after surgery. Subcutaneous fat was removed, and skin was cut in 1.5 × 1.5 cm squares. For serine protease treatment, the skin was first cleaned with 50 μL of $CHCl_3/CH_3OH$ (1:1) dropped on a Finn chamber paper disc and placed for 1 min on the top of the skin sample. Then, the skin was exposed to 20 μL of a 0.15 mg/mL solution of serine protease (pig pancreas trypsin, Biochrom, Berlin, Germany) for different time periods (2, 4, 8, and 16 h). Control skin samples were treated with 20 μL of 0.9% sterile saline. After incubation, the remaining solution was removed from the skin surface by a cotton swab. The following formulations were applied for systematic drug penetration studies: (i) 40 μL/cm^2 of a 2.5 μg/mL rapamycin solution in 36% ethanol, leading to a final amount of 100 μg/cm^2 rapamycin deposited on the skin and incubated for variable time periods (10, 100, and 1000 min, respectively); (ii) 50 μL/cm^2 of 8.5 mg/mL rapamycin dissolved in 70% ethanol and 2.5% hydroxyethyl cellulose (HEC) gel leading to a final amount of 425 μg/cm^2 deposited on the skin. Note that previous work indicates that HEC gel does not change the penetration properties, but it avoids drying of the drug on the skin surface at long penetration times and high drug loads.[25] Some of the skin samples exposed to the HEC gel formulation were pretreated with trypsin for variable time periods (20 μL/cm^2 of a 0.15 μg/mL solution) of 2, 4, 8, and 16 h, respectively. Similar to previous work, this pretreatment was performed to model the enzymatic activity, cytokine environment, and barrier alteration typical of inflamed skin.[38,39] The samples were treated with a cotton swab for removing the formulation still sticking to the skin surface and subsequently prepared for

https://doi.org/10.1021/acsomega.1c01058
ACS Omega 2021, 6, 12213−12222

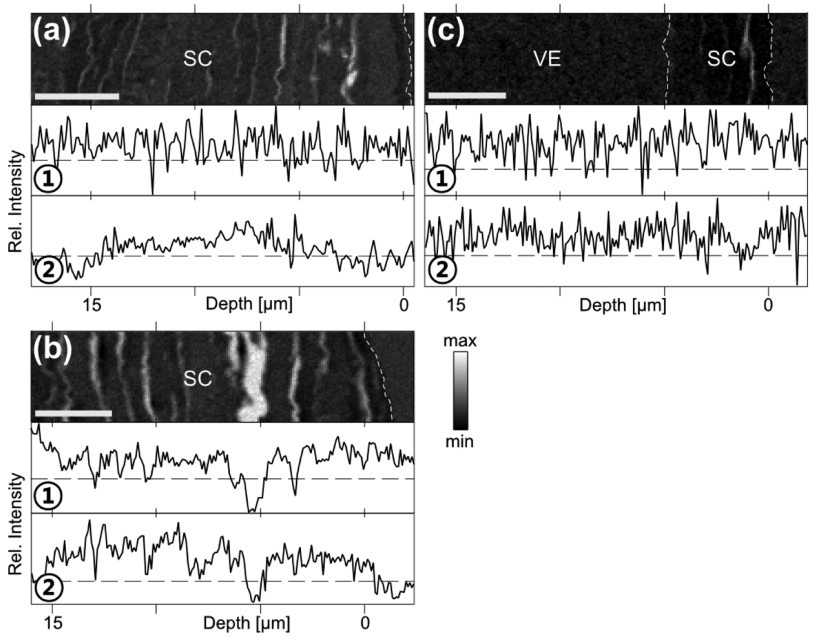

Figure 2. Penetration of rapamycin dissolved in ethanol (100 μg/cm^2) topically applied to human SC ex vivo. Top: X-ray micrograph at 532.03 eV (white color corresponds to high transmission, black color to low transmission, see also included scheme of grayscale between the minimum (min) and maximum (max) of X-ray transmission), middle: rapamycin distribution as a function of skin depth at the same depth scale as the X-ray micrographs using 531.14 and 530.74 eV (approach 1, labeled ①); bottom: results from singular value decomposition (approach 2, labeled ②): (a) 10 min penetration time; (b) 100 min penetration time; and (c) 1000 min penetration time. The dashed thin white lines in the micrographs mark the top of the SC, that is, the skin surface is on the right-hand side. In (c), the top of the VE is also marked by another white dashed line. The scale bars correspond to 4 μm. The skin surface at the top edge of each micrograph is chosen as the reference of the depth scale. Horizontal black dashed lines are used to guide the eye for the depth profiles of rapamycin. The minimum (min) and maximum (max) correspond to (a) 80,000 and 175,000; (b) 68,500 and 179,500; (c) 67,000 and 127,500 counts/s, respectively.

STXM studies by fixation in 2.5% glutaraldehyde and 1% cacodylate buffer. Finally, they were embedded in EPON resin (Serva, Heidelberg, Germany) and cut into 200−300 nm slices with an area of typically 500 μm × 500 μm using an ultramicrotome, similar to previous work.[24−26,28,45−47] The samples were deposited on silicon nitride (Si_3N_4) windows (thickness: 100 nm, Silson, UK). All samples were characterized by optical microscopy (MM-400/LU, Nikon) prior to the STXM studies for selecting distinct regions to be investigated. The thickness of the samples was subsequently measured by AFM (nanoIR-2s, Anasys) in those regions that were studied by STXM.

The STXM studies were performed at the beamline BL4U at UVSOR-IIII Synchrotron (Institute for Molecular Science, Okazaki, Japan).[48] UVSOR-III is operated at 750 MeV and 300 mA in the top-up injection mode. The STXM (Research Instruments, ex Bruker) at BL4U uses a Fresnel zone plate (FZP, Applied Nanotools, Edmonton, Canada) as the focusing optical element. The design of the FZP is optimized for the O 1s regime (520−565 eV). Its parameters are a diameter of 300 μm and an outermost zone width of 18 nm, and the nickel pattern on a Si_3N_4 membrane substrate is 50 nm thick. The focal length is 2.3 mm at 530 eV. The photon energy scale was calibrated by the O 1s → π^* transitions of CO_2 and dexamethasone.[24,49] The energy resolution was adjusted by the width of the slits of the X-ray monochromator of typically 50 μm, corresponding to an energy resolution of ∼60 meV at the O 1s edge. The width of the slit also determines the focusing spot size at the sample corresponding to 74 nm in the O 1s regime. The STXM was operated in the on-the-fly mode for scans with a squared pixel size of 250 nm for overview images of the top skin layers, 100 nm for detailed scans of the SC, and 30 nm for high-resolution scans at a dwell time per pixel of 4 ms. Typical areas covered by each scan were 50 μm × 10 μm, 20 μm × 5 μm, and 4 μm × 2 μm, respectively. The soft X-ray monochromator was used with variable energy step widths, covering 134 maps per stack of each experiment between 520 and 565 eV. This allows us to have sufficiently small energy steps of 0.1 eV for gathering the near-edge features, whereas in the pre-edge- and post-edge-continua, the energy step width varied between 0.5 and 0.607 eV, respectively. This approach is different from our previous work, where only a few photon energies were selected during the experiments due to long data acquisition times and limited beam time.[24−26] As a result, the analysis of the optimum X-ray contrast can be done in the present experiments during the detailed data analysis, that is, after the beam time. Radiation damage is only observed for repeated scans at the same location, as evidenced by bleaching of the samples in multiple scanned areas.

Positional shift of the raw stacks of X-ray absorption spectra was corrected for lateral drifts using the Zimba tool in the aXis2000 program.[50] Small energy shifts of the order of <200 meV, occurring during data acquisition of the spectral stacks, were identified from the total absorption signal using the known X-ray absorption of dexamethasone.[24] These corrections were considered for both approaches of data evaluation outlined in the following so that the results can be compared to each other, especially since they are extracted from the same raw data. The optical density $\ln(I_0/I)$ can be used to determine the local concentration and the fraction of penetrated drug relative to the topically applied drug, according to the Beer−

https://doi.org/10.1021/acsomega.1c01058
ACS Omega 2021, 6, 12213−12222

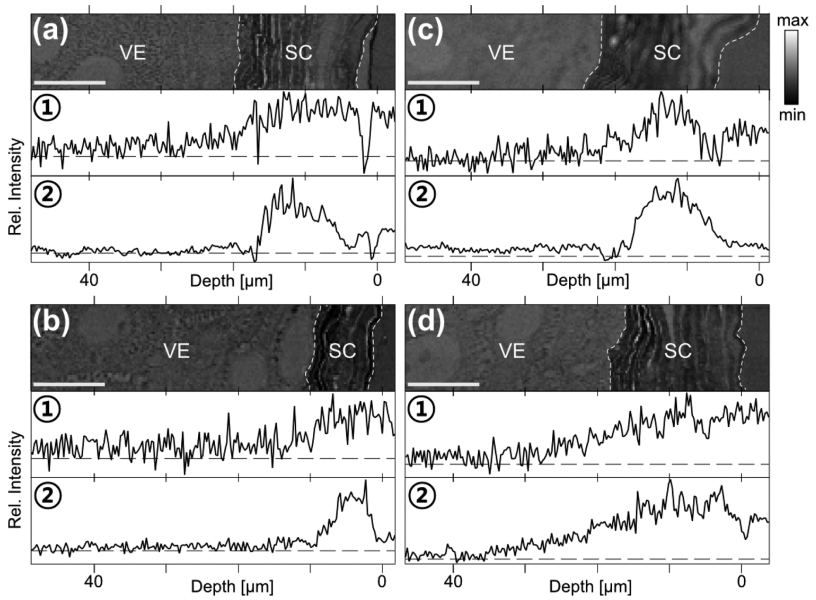

Figure 3. Penetration of rapamycin dissolved in HEC gel (rapamycin: 425 μg/cm^2 topically applied to the skin for 24 h). Top: X-ray micrographs at 532.03 eV; middle (approach 1, labeled ①): rapamycin distributions as a function of skin depth on the same length scale as the X-ray micrographs using the same photon energies as specified in Figure 2; bottom (approach 2, labeled ②): rapamycin distributions derived from singular value decomposition as a function of skin depth on the same length scale as the X-ray micrographs: (a) 2 h primary preparation with serine protease; (b) 4 h primary preparation with serine protease; (c) 8 h primary preparation with serine protease; and (d) 16 h primary preparation with serine protease. The vertical dashed thin white line on the right-hand side of each micrograph marks the skin surface. The left vertical dashed line corresponds to the top of the VE, which is located below the SC. The scale bar corresponds to 10 μm. The skin surface at the top edge of each micrograph is chosen as the reference of the depth scale. The dashed black horizontal lines in the rapamycin distributions as a function of depth are inserted to guide the eye. The minimum (min) and maximum (max) correspond to (a) 970,000 and 1,385,000; (b) 900,000 and 1,315,000; (c) 980,000 and 1,365,000; and (d) 942,500 and 1,445,000 counts/s, respectively.

Lambert law, similar to previous work:[24−26,47] $\ln(I_0/I) = \sigma \cdot c \cdot d$, where I_0 is the intensity of the incident photons, I is the intensity of the transmitted photons, σ is the absorption cross section (in Mbarn, 1 Mbarn corresponds to 10^{-18} cm^2, see Figure 1), c is the concentration of the absorber, and d is the thickness of the sample absorbing X-rays, as determined by AFM. I_0 is obtained from appropriate reference spectra, that is, the transmitted radiation without the absorbing skin sample in the photon beam. Reference spectra were frequently recorded for taking any temporal changes in photon flux into account. Absolute absorption cross sections were derived at 560 eV using tabulated reference data.[51]

The STXM data were analyzed in two different ways, where the former is similar to previous work,[24−26,47] by using two-photon energies, where the X-ray absorption cross section of the species to be detected is different and can be distinguished from the fixed skin matrix through its absorption cross section and chemical shift even in small concentrations. This corresponds to approach 1 and is also labeled as ① in Figures 2−4. For probing rapamycin, we used the photon energies 531.13 and 530.73 eV (cf. Figure 1). These energies turned out to be the most sensitive for probing the drug in fixed human skin. Small changes in photon energy occurring during data acquisition, which are due to slight changes in optical element position in the monochromator or electron beam position in the storage ring, were corrected for the data stacks evaluated. These photon energies yield for rapamycin a change in absorption cross section of 6 ± 0.5 Mbarn (cf. Figure 1), whereas the absorption cross sections of EPON resin and fixed skin remain fairly constant at both photon energies.

Alternatively, the O 1s spectral shapes of the different components contributing to the X-ray absorption signal have been deconvoluted using a linear combination of a limited number of spectral components of the major species contained in the skin samples, requiring reliable reference spectra for

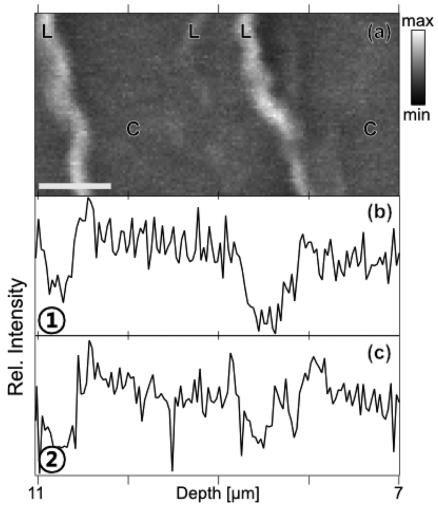

Figure 4. (a) High-resolution X-ray micrograph recorded at 532.03 eV in the SC of a skin sample exposed for 16 h to trypsin and subsequently for 1000 min to an ethanolic rapamycin solution. Lipid layers are marked by L and corneocytes by C. Pixel size: 30 nm^2; the scale bar corresponds to 800 nm. The skin surface is chosen as the reference of the depth scale. (b) Integrated intensity of the rapamycin concentration on the same length scale as the micrograph using approach 1 (labeled ①) and (c) integrated intensity of the rapamycin concentration on the same length scale as the micrograph using approach 2 (labeled ②). The minimum (min) and maximum (max) correspond to 246,000 and 472,000 counts/s, respectively.

https://doi.org/10.1021/acsomega.1c01058
ACS Omega 2021, 6, 12213−12222

these major species in the investigated samples. It is similar to that used along with STXM, for example, for analyzing polymer blends.[52] We also note that there are also program packages, such as MANTiS, available.[53] However, the present analysis goes beyond with respect to the control of parameters, such as avoidance of negative concentrations and exact energy calibration of the data stacks and reference spectra, which is crucial for the identification of low concentrations of the penetrated drug. This approach 2 is labeled as ② in Figures 2−4. It is evident that the fixed skin contains a large number of chemical compounds, which cannot be considered by such an approach. Therefore, we grouped them together as follows: (i) rapamycin, the drug to be identified; (ii) human skin, which varies its composition as a function of depth. Therefore, these variations are considered by changes in cross section in the O 1s → π^* and O 1s → σ^* regimes. These quantities reflect local changes in skin composition which vary due to a different degree of unsaturated and saturated moieties in the skin samples probed by element-specific O 1s excitation, for example, accounting for different chemical compositions in the SC, where corneocytes and the lipid lamellae have different X-ray absorption spectra, as well as the viable epidermis (VE); and (iii) EPON resin, which is used for embedding the skin samples. These reference spectra are shown in the Supporting Information (see Figure S1). This implies that the interactions between the biological matrix and the drug do not have any significant influence on the shape of the X-ray absorption spectra.

The weight factors of the individual components of data analysis in approach 2 were obtained from a program written in Igor Pro 8 (WaveMetrics, Lake Oswego, OR, U.S.A.) using a Levenberg−Marquardt algorithm that minimizes the deviations of the weighted sum of the reference spectra from the experimental absorption spectrum contained in each pixel. From these weight factors, the local concentrations of the major components are derived by considering the local thickness of the sample, which was determined from supplementary AFM measurements. Significant changes in skin thickness were especially probed in the SC, where corneocytes are often thicker than the lipid regions between them. This is accomplished by measuring the height of the EPON resin by AFM in the same regions scanned by STXM. As a result, one can derive the local concentration of the drug rapamycin in the skin sections under study using both approaches. Finally, penetration profiles of rapamycin were derived by integrating each line of the maps, corresponding to a given depth below the skin surface, for each component. Here, we focus on the local drug distribution, but this approach can also be applied to any component contained in the skin sections. Note that approach 2 is more sensitive to spatial drifts of the sample due to the substantial data acquisition times, which range typically between 30 and 60 min per stack. This is different from approach 1, in which the energies used for probing rapamycin are only separated by 400 meV so that in this case, no spatial shifts of the sample occur.

RESULTS AND DISCUSSION

Figure 1 shows the absorption cross section of rapamycin in the O 1s regime along with its structure ($C_{51}H_{79}NO_{13}$, M = 914.17 g/mol, see the inset of Figure 1). This is the origin of selective and quantitative probing of this drug. The absolute absorption cross-sectional scale is calibrated at 560 eV, that is, far above the broad O 1s → σ^* transition, where the continuum cross section dominates using the known atomic absorption cross section according to tabulated data.[51] Note that the underlying cross section from the valence shell as well as the C 1s and N 1s continua has been subtracted so that only the O 1s specific cross section is shown in Figure 1.

The spectral features of selective O 1s excitation are reported, indicating an intense and slightly asymmetric O 1s → π^* transition peaking at 531.2 eV [see Figure 1, inset (a)]. This feature is slightly asymmetrically broadened due to different chemical shifts at different carbonyl and carboxyl sites.[49,54] The lower energy part of this resonance at 531.13 eV is used for selective probing of rapamycin in human skin. This is essentially due to the carbonyl oxygen sites, similar to previous work on dexamethasone.[24] The carboxyl site is expected to occur at the high energy part of the O 1s → π^* -resonance.[49] The other intense feature is the broad O 1s → σ^* transition peaking at 539.5 eV with an absorption cross section of 15 Mbarn.

Figure 2 shows a series of X-ray micrographs taken at 532.03 eV at the top of each figure, where the transmitted X-rays provide the contrast. This photon energy was chosen due to its high X-ray contrast, visualizing the structural features of the top skin layers, mostly showing the SC with its stratified structure of corneocytes. Note that the skin surface is located on the right-hand side and the depth increases to the left. This orientation of the skin samples was chosen for instrumental reasons so that during data acquisition, each line scanned horizontally corresponds to a depth profile. Only for 1000 min penetration time, the stratified structures appear to be significantly thinner (see Figure 2c), which is most likely due to alterations of this top skin layer as a result of the long penetration time and exposure to the drug formulation containing ethanol. The thin white structures in the SC correspond to the lipid layers between the corneocytes. They can be as thin as ∼100 nm and have been easily resolved by high-resolution scans of STXM.[25] Previous work has indicated that in these layers most hydrophobic drugs, such as dexamethasone, were found, whereas no drugs were found in the corneocytes.[25] Similarly, we would expect that rapamycin should also be preferably found in these lipid layers, even if drug penetration is inefficient. The reason for this expectation is that rapamycin has even higher octanol−water distribution coefficient log P (log P = 4.3)[35] than dexamethasone (log P = 1.83).[35] The penetration time of the topically applied ethanolic rapamycin solution depositing 100 μg/cm^2 of the drug is varied ranging from 10 (a) over 100 (b) to 1000 min (c). Rapamycin is probed in the graphs marked by ① according to approach 1, that is, at 531.13 and 530.73 eV (see Experimental Section). Then, these changes in optical density, recorded at both photon energies, are subtracted pixel by pixel and subsequently integrated line by line, that is, as a function of depth. This yields, on a relative scale, the drug concentration as a function of depth (labeled ① in Figure 2a−c). These signals appear to be flat and noisy, similar to previous work, if no drug has penetrated the skin.[24,25,47] We note that the topically deposited drug concentration was not too low to be detected since, in other experiments communicated below, the topically applied ethanol solution of rapamycin is clearly detected after primary treatment with serine protease.

None of the integrated signals, corresponding to the local rapamycin concentration as a function of depth, shows any evidence for a local increase in drug concentration, which means that the drug is not probed by approach 1 no matter

https://doi.org/10.1021/acsomega.1c01058
ACS Omega 2021, 6, 12213−12222

how long the intact skin is exposed to the drug formulation, that is, $t \leq 16$ h. The same result is obtained from the singular value decomposition (approach 2), marked by ② in Figure 2. Only small differences occur between both approaches, for example, in Figure 2b; a distinct minimum, corresponding to a defect in the skin, is observed more distinctly using approach 1, but it is less pronounced in approach 2. Overall, both approaches used to evaluate the penetration of ethanolic rapamycin solution yield the same result, that is, no drug penetrated intact skin if the penetration time of the ethanolic drug solution is increased up to 1000 min. This result is remarkable since it is known that ethanol is not only the solvent for rapamycin, but it also acts as a penetration enhancer.[20] These results serve as an important benchmark for determining the role of serine protease with respect to changes in penetration properties of rapamycin and the accompanied changes in the skin barrier, which are discussed in the following.

Figure 3 shows the results of a series of experiments, covering the SC and the top part of the VE, in which the skin was topically pretreated with the serine protease trypsin for defined time periods ranging between 2 and 16 h. Subsequently, the HEC gel drug formulation was topically applied to the prepared skin sections for 24 h (1440 min) at a concentration of 425 μg/cm^2. Rapamycin was probed in the same way as shown in Figure 2, that is, by approaches 1 and 2. The results shown in Figure 3a clearly indicate that after 2 h of pretreatment with trypsin, there is from both approaches a visible enhancement of rapamycin in the SC, whereas, in the VE, no drug is observed, as visualized by a horizontal dashed line for both approaches. Note that the drug distributions derived from these approaches are similar but not identical. The signal-to-noise ratio from the evaluation employing approach 1 is lower, and the drug appears to be more continuously distributed in the entire SC, whereas the drug distribution derived from singular value decomposition (approach 2) is substantially more pronounced, as indicated by a higher signal-to-noise level in the local drug concentration. This finding is explained by the fact that approach 2 makes use of the entire spectral data gathered in the O 1s-regime, whereas approach 1 only considers two-photon energies.

Circular structures are observable in the VE and are due to the nuclei of keratinocytes. These are not involved in drug uptake, since it is likely that the tight junction barrier remains intact after 2 h exposure to trypsin. This result is ascribed to the efficacy of trypsin to alter the barrier of the top skin layer at least after a short treatment time of the SC (e.g., 2−8 h), allowing rapamycin to enter only this top skin layer. The sharp minimum in local drug concentration probed by both approaches 1 and 2 near the skin surface is due to a loose layer of corneocytes (see Figure 3a) that is not any more connected to the compact SC.

There are some differences in drug distribution derived from both approaches. Approach 1 yields a noisy and continuous drug distribution, whereas from approach 2, detailed structures are derived. Even at a low spatial resolution, it is evident that the local maxima in rapamycin concentrations are observed in the corneocytes, especially in the lower SC, whereas minima are connected with the lipid layers between the corneocytes. This result is quite unexpected as compared to previous work on dexamethasone, which was exclusively found in the lipid layers.[25] Also, polymer core-multishell nanocarriers with sizes below 10 nm were also observed in these thin lipid layers.[26]

We rationalize the present result in terms of a significant loss of the integrity of the upper SC induced by trypsin in the top skin barrier. This is connected to the structure of corneocytes where a thin corneocyte lipid envelope and a cornified cell envelope are present inside the intercellular lipid layers.[55] Earlier NMR studies have indicated that the lipids are covalently bound to the protein envelope.[56] Inside the corneocyte keratins, filaggrins and their degradation products are found, consisting of serine, glycine, and glutamine in filaggrins.[57] It appears to be straightforward to assume that a loss of the thin corneocyte envelope barrier induced by serine protease will provide access to trypsin to the bulk interior of the corneocytes to cleaving the serine moieties, which are known to contribute to 25.3% of the filaggrin.[57] The subsequently applied rapamycin formulation can then penetrate corneocytes. As a consequence, rapamycin can penetrate the entire SC but not the VE after 2 h of exposure to trypsin, implying that the tight junction barrier in the stratum granulosum remains still intact. We also observe an increase in drug concentration right above the skin surface. This is ascribed to residues of the drug that is still sticking to the skin surface and is not fully removed by a cotton swab done prior to fixation of the skin samples. This situation is not significantly different if the exposure time to trypsin is increased to 4 and 8 h (see Figure 3b,c), respectively. The SC appears to be specifically thin in the analyzed region of Figure 3b. Therefore, the amount of the drug appears to be low, but there is also no drug observed in the VE via approaches 1 and 2. In the sample, corresponding to 8 h of trypsin exposure shown in Figure 3c, the drug is broadly distributed over the SC, as follows from both approaches. However, in the lowest part of this layer, apparently no or little drug is found. These variations observed for the samples analyzed in Figure 3b,c can be due to local variability of trypsin and subsequent drug applications that cannot be easily controlled prior to analysis, even though the same protocol was followed. This situation appears to be different after 16 h exposure to trypsin (see Figure 3d). The drug is broadly spread, but the distribution is rather homogeneous not only in the SC but also in the VE, as follows from both approaches of data analysis. Spatially resolved results from approach 2 indicate that rapamycin is diffusely spread over the top part of the VE (see also Supporting Information, Figure S8a). This implies that longer time periods of serine protease treatment may be associated with damage to the tight junctions, which are known to be located in the stratum granulosum, by trypsin, so that rapamycin can penetrate to deeper skin layers. More specifically, the tight junctions of the stratum granulosum contain occludin.[58] This protein contains serine moieties,[59] which can be affected by trypsin. This suggests that diffusive penetration of topically applied trypsin takes more than 8 h to reach and disturb the tight junctions in the stratum granusolum. The present finding is also consistent with earlier ones that drug penetration is enhanced in inflamed skin.[60] However, this is different from studies on the penetration of polymer nanocarriers that were not affected by inflammation.[61]

Figure 4a shows a high-resolution X-ray micrograph taken in the middle of the SC recorded at 532.03 eV. This skin sample has been exposed for 16 h to trypsin and subsequently for 1000 min to an ethanolic rapamycin solution (100 μg/cm^2). Note that without the pretreatment with trypsin, no drug

https://doi.org/10.1021/acsomega.1c01058
ACS Omega 2021, 6, 12213−12222

penetration was observed under these conditions (cf. Figure 2c). Pretreatment of the skin samples with serine protease is evidently of importance for rapamycin penetration, as was shown in the results shown in Figure 3. This means that the drug formulation is of minor importance for drug penetration. Figure 4a shows corneocytes (C) (gray areas) and the vertical less absorbing bright thin regions are attributed to the lipid layers (L) separating the corneocytes. Their internal structure is known from high-resolution electron microscopy[37,62] but cannot be fully resolved by STXM.[25] Figure 4b,c shows the integrated intensity of the rapamycin concentration in this part of the skin sample using approaches 1 and 2, respectively.

Both approaches yield the same result for the lipid structures with a width ranging between 130 and 300 nm. The minima in local rapamycin concentration coincide with the prominent lipid structures, whereas the highest local drug concentration is found in the area of corneocytes. This result underscores the conclusions derived from low spatial resolution studies (see Figure 3) and is unlike the expectation that lipophilic drugs should be preferentially located in the lipid layers, as was observed for dexamethasone from X-ray microscopy.[25] Evidently, the corneocytes become accessible to drug penetration via the pretreatment with trypsin. The present results also suggest that there is a diffusive transport from the lipid layers between the corneocytes into the bulk interior of the corneocytes so that the concentration in the lipid layers is decreased. The exact details of these changes are not clear to the best of our knowledge and require further work.

Finally, the amount of the penetrated rapamycin is quantified using approaches 1 and 2 of data evaluation since X-ray microscopy provides quantitative information on dermal drug penetration.[24−26] The mass of the applied drug was always 425 ± 5 $\mu g/cm^2$. According to approach 1, the integrals of the relative drug intensities shown in Figure 3 are used, yielding the mass of the drug penetrating the skin samples. Similarly, approach 2 is also used for determining the drug uptake into the skin samples. Here, the relative weight factors are used accordingly. The results are shown on a relative scale in percent of the topically applied rapamycin that is found in the top skin layers (see Table 1), which can be easily transferred to an absolute mass scale by considering the topically applied amount of the drug. In general, both approaches yield a similar temporal evolution, even though the relative uptake derived from approach 1 appears to be systematically somewhat smaller than those derived from approach 2. The higher values from approach 2 are considered to be more reliable since the entire spectral information is used for evaluation, rather than two micrographs taken at close-lying photon energies. We also conclude from this result that earlier work derived according to approach 1 can also be considered to be correct.[24−26,47] However, approach 2 appears to be preferred, specifically for highly dilute absorbers that have no chemical shift of the resonant transitions, such as the O 1s → π^* transition compared to the majority species, that is, EPON resin and the skin matrix. Further evidence for this conclusion comes from supplementary work on model skin, where the results from STXM were compared to other analytical approaches.[46] The present results also indicate that a distinctly lower drug uptake is derived for the sample that was exposed for 4 h to serine protease, where the SC is significantly thinner than for the other samples (see Figure 3). If normalized to the thickness of the SC, one derives for this sample an almost identical value as for the other ones at 2 and 8 h. As a result, no clear trend is observed for the investigated treatment times with serine protease. This may imply that 2 h of trypsin treatment prior to topical drug penetration are sufficient to make the SC accessible to rapamycin, whereas longer times periods are required to damage the tight junction barrier so that rapamycin can even penetrate the VE, as observed for 16 h pretreatment with trypsin, which yields the highest drug uptake for both approaches. Compared to the ethanolic formulation without trypsin pretreatment that does not show any increase in local drug concentration near the skin surface, we can conclude that the serine protease trypsin increases the drug penetration of rapamycin significantly with a drug uptake reaching 58 ± 2% at 16 h of pretreatment time as derived from approach 2 and 42 ± 5% according to approach 1. This implies that drugs exceeding the 500 Da limit can be absorbed in the skin if the skin barrier is significantly weakened. This underscores that treatment with serine protease is suitable to simulate inflammations in skin samples ex vivo.

Table 1. Fraction of the Topically Applied Rapamycin to Human Skin after Modification of the Skin Barrier by the Serine Protease Trypsin for Variable Time Periods, Followed by 24 h Exposure to a Formulation of Rapamycin in HEC Gel

exposure time of skin sample to serine protease [h]	mass of topically applied rapamycin [$\mu g/cm^2$]	fraction of rapamycin probed in skin [%] by approach 1	fraction of rapamycin probed in skin [%] by approach 2
2	425 ± 5	31 ± 5	43 ± 6
4	425 ± 5	11 ± 5	11 ± 2
8	425 ± 5	32 ± 5	44 ± 7
16	425 ± 5	42 ± 5	58 ± 2

CONCLUSIONS

The present results indicate that STXM is capable of probing selectively and quantitatively the immunosuppressive drug rapamycin in human skin ex vivo. This is possible on the one hand due to a slight chemical shift of the O 1s → π^* transition of rapamycin, which is different from that of the other majority species contained in fixed human skin. On the other hand, the approach of singular value decomposition makes use of the full spectral information gathered in each pixel of the X-ray micrographs and yields comparable results to the other approach. This work is from the methodological point of view primarily devoted to demonstrating the equivalence of both approaches of data evaluation. However, the full potential of singular value decomposition is exploited, if the drug or other species of interest shows no chemical shifts relative to the majority species contained in fixed skin so that it becomes impossible to use just two-photon energies, corresponding to approach 1. Such studies go beyond the scope of this work and will be the subject of subsequent work.

From the dermatological point of view, it is shown that an ethanolic drug solution does not increase the skin penetration of a lipophilic high-molecular-weight drug, which is fully consistent with the 500 Da rule. Topically applied rapamycin only penetrates intact human skin, if the skin barrier is weakened by pretreatment with the serine protease trypsin. Upon enzymatic disruption of the SC barrier, the topically applied drug is mostly distributed in the SC. High spatial resolution experiments indicate that rapamycin is primarily found in corneocytes but not in the lipid layers between the

https://doi.org/10.1021/acsomega.1c01058
ACS Omega 2021, 6, 12213−12222

corneocytes. This behavior is rationalized in terms of chemical changes to the skin lipids and corneocytes induced by serine protease. Furthermore, long exposure times to trypsin indicate that rapamycin can also penetrate the VE. Further experiments will investigate if this result can be assigned to the damage of the tight junction barrier, which requires serine protease penetration to the deepest layers of the SC and thus longer incubation times.

■ ASSOCIATED CONTENT

Supporting Information

The Supporting Information is available free of charge at https://pubs.acs.org/doi/10.1021/acsomega.1c01058.

Singular value decomposition, reference spectra, and spatial distribution of the spectral components of the samples shown in Figures 2−4 (PDF)

■ AUTHOR INFORMATION

Corresponding Author

Eckart Rühl − *Physical Chemistry, Freie Universität Berlin, Berlin 14195, Germany;* orcid.org/0000-0002-0451-8734; Email: ruehl@zedat.fu-berlin.de

Authors

Gregor Germer − *Physical Chemistry, Freie Universität Berlin, Berlin 14195, Germany*

Takuji Ohigashi − *UVSOR Synchrotron Facility, Institute for Molecular Science, Okazaki 444-8585, Japan*

Hayato Yuzawa − *UVSOR Synchrotron Facility, Institute for Molecular Science, Okazaki 444-8585, Japan;* orcid.org/0000-0003-4129-4407

Nobuhiro Kosugi − *UVSOR Synchrotron Facility, Institute for Molecular Science, Okazaki 444-8585, Japan;* orcid.org/0000-0003-2069-9122

Roman Flesch − *Physical Chemistry, Freie Universität Berlin, Berlin 14195, Germany*

Fiorenza Rancan − *Charité-Universitätsmedizin, Berlin 10117, Germany;* orcid.org/0000-0003-3903-3240

Annika Vogt − *Charité-Universitätsmedizin, Berlin 10117, Germany*

Complete contact information is available at: https://pubs.acs.org/10.1021/acsomega.1c01058

Notes

The authors declare no competing financial interest.

■ ACKNOWLEDGMENTS

We thank the staff of the UVSOR facility for their great support of this work. Financial support by DFG (RU420/12-1, VO 926/3-1) and JSPS (JP17H03013) is gratefully acknowledged. We acknowledge the support of the Open Access Publication Fund of the Freie Universität Berlin.

■ REFERENCES

(1) Trommer, H.; Neubert, R. H. H. Overcoming the stratum corneum: The modulation of skin penetration—A review. *Skin Pharmacol. Physiol.* **2006**, *19*, 106−121.

(2) Proksch, E.; Brandner, J. M.; Jensen, J.-M. The skin: an indispensable barrier. *Exp. Dermatol.* **2008**, *17*, 1063−1072.

(3) Elias, P. M. Stratum corneum defensive functions: An integrated view. *J. Invest. Dermatol.* **2005**, *125*, 183−200.

(4) Parisi, R.; Symmons, D. P. M.; Griffiths, C. E. M.; Ashcroft, D. M.; Identification, M. Global Epidemiology of Psoriasis: A Systematic Review of Incidence and Prevalence. *J. Invest. Dermatol.* **2013**, *133*, 377−385.

(5) Leung, D. Y. M.; Boguniewicz, M.; Howell, M. D.; Nomura, I.; Hamid, Q. A. New insights into atopic dermatitis. *J. Clin. Invest.* **2004**, *113*, 651−657.

(6) Bos, J. D.; Meinardi, M. M. H. M. The 500 Dalton rule for the skin penetration of chemical compounds and drugs. *Exp. Dermatol.* **2000**, *9*, 165−169.

(7) Dheer, D.; Jyoti; Gupta, P. N.; Shankar, R. Tacrolimus: An updated review on delivering strategies for multifarious diseases. *Eur. J. Pharm. Sci.* **2018**, *114*, 217−227.

(8) Peramo, A.; Marcelo, C. L. Visible effects of rapamycin (sirolimus) on human skin explants in vitro. *Arch. Dermatol. Res.* **2013**, *305*, 163−171.

(9) Motzer, R. J.; Escudier, B.; Oudard, S.; Hutson, T. E.; Porta, C.; Bracarda, S.; Grünwald, V.; Thompson, J. A.; Figlin, R. A.; Hollaender, N.; Urbanowitz, G.; Berg, W. J.; Kay, A.; Lebwohl, D.; Ravaud, A. Efficacy of everolimus in advanced renal cell carcinoma: a double-blind, randomised, placebo-controlled phase III trial. *Lancet* **2008**, *372*, 449−456.

(10) Tu, J.; Foster, R. S.; Bint, L. J.; Halbert, A. R. Topical rapamycin for angiofibromas in paediatric patients with tuberous sclerosis: Follow up of a pilot study and promising future directions. *Australas. J. Dermatol.* **2014**, *55*, 63−69.

(11) Le Guyader, G.; Vieillard, V.; Andrieux, K.; Rollo, M.; Thirion, O.; Wolkenstein, P.; Paul, M. Long-term stability of 0.1% rapamycin hydrophilic gel in the treatment of facial angiofibromas. *Eur. J. Hosp. Pharm.* **2020**, *27*, e48−e52.

(12) Chen, P. L.; Hong, J. B.; Shen, L. J.; Chen, Y. T.; Wang, S. J.; Liao, Y. H. The efficacy and safety of topical rapamycin-calcitriol for facial angiofibromas in patients with tuberous sclerosis complex: a prospective, double-blind, randomized clinical trial. *Br. J. Dermatol.* **2020**, *183*, 655−663.

(13) Wataya-Kaneda, M.; Nagai, H.; Ohno, Y.; Yokozeki, H.; Fujita, Y.; Niizeki, H.; Yoshida, K.; Ogai, M.; Yoshida, Y.; Asahina, A.; Fukai, K.; Tateishi, C.; Hamada, I.; Takahata, T.; Shimizu, K.; Shimasaki, S.; Murota, H. Safety and Efficacy of the Sirolimus Gel for TSC Patients With Facial Skin Lesions in a Long-Term, Open-Label, Extension, Uncontrolled Clinical Trial. *Dermatol. Ther.* **2020**, *10*, 635−650.

(14) Kim, D.-H.; Sarbassov, D. D.; Ali, S. M.; King, J. E.; Latek, R. R.; Erdjument-Bromage, H.; Tempst, P.; Sabatini, D. M. MTOR interacts with Raptor to form a nutrient-sensitive complex that signals to the cell growth machinery. *Cell* **2002**, *110*, 163−175.

(15) Hara, K.; Maruki, Y.; Long, X.; Yoshino, K.-i.; Oshiro, N.; Hidayat, S.; Tokunaga, C.; Avruch, J.; Yonezawa, K. Raptor, a binding partner of target of rapamycin (TOR), mediates TOR action. *Cell* **2002**, *110*, 177−189.

(16) Zheng, Y.; Yu, J. mTOR Inhibitors at a Glance. *Mol. Cell. Pharmacol.* **2016**, *7*, 15−20.

(17) Zaza, G.; Granata, S.; Caletti, C.; Signorini, L.; Stallone, G.; Lupo, A. mTOR Inhibition Role in Cellular Mechanisms. *Transplantation* **2018**, *102*, S3−S16.

(18) Dias, V. C.; Yatscoff, R. W. Investigation of Rapamycin Transport and Uptake Across Absorptive Human Intestinal Cell Monolayers. *Clin. Biochem.* **1994**, *27*, 31−36.

(19) Haidinger, M.; Poglitsch, M.; Geyeregger, R.; Kasturi, S.; Zeyda, M.; Zlabinger, G. J.; Pulendran, B.; Hörl, W. H.; Säemann, M. D.; Weichhart, T. A Versatile Role of Mammalian Target of Rapamycin in Human Dendritic Cell Function and Differentiation. *J. Immunol.* **2010**, *185*, 3919−3931.

(20) Williams, A. C.; Barry, B. W. Penetration enhancers. *Adv. Drug Delivery Rev.* **2004**, *56*, 603−618.

(21) Sukhanova, A.; Devy, J.; Venteo, L.; Kaplan, H.; Artemyev, M.; Oleinikov, V.; Klinov, D.; Pluot, M.; Cohen, J. H. M.; Nabiev, I. Biocompatible fluorescent nanocrystals for immunolabeling of membrane proteins and cells. *Anal. Biochem.* **2004**, *324*, 60−67.

(22) Betzig, E.; Patterson, G. H.; Sougrat, R.; Lindwasser, O. W.; Olenych, S.; Bonifacino, J. S.; Davidson, M. W.; Lippincott-Schwartz,

J.; Hess, H. F. Imaging intracellular fluorescent proteins at nanometer resolution. *Science* **2006**, *313*, 1642−1645.
(23) Zhang, D.; Bian, Q.; Zhou, Y.; Huang, Q.; Gao, J. The application of label-free imaging technologies in transdermal research for deeper mechanism revealing. *Asian J. Pharm. Sci.* **2020**, DOI: 10.1016/j.ajps.2020.07.004.
(24) Yamamoto, K.; Flesch, R.; Ohigashi, T.; Hedtrich, S.; Klossek, A.; Patoka, P.; Ulrich, G.; Ahlberg, S.; Rancan, F.; Vogt, A.; Blume-Peytavi, U.; Schrade, P.; Bachmann, S.; Schäfer-Korting, M.; Kosugi, N.; Rühl, E. Selective probing of the penetration of dexamethasone into human skin by soft X-ray spectromicroscopy. *Anal. Chem.* **2015**, *87*, 6173−6179.
(25) Yamamoto, K.; Klossek, A.; Flesch, R.; Rancan, F.; Weigand, M.; Bykova, I.; Bechtel, M.; Ahlberg, S.; Vogt, A.; Blume-Peytavi, U.; Schrade, P.; Bachmann, S.; Hedtrich, S.; Schäfer-Korting, M.; Rühl, E. Influence of the skin barrier on the penetration of topically-applied dexamethasone probed by soft X-ray spectromicroscopy. *Eur. J. Pharm. Biopharm.* **2017**, *118*, 30−37.
(26) Yamamoto, K.; Klossek, A.; Flesch, R.; Ohigashi, T.; Fleige, E.; Rancan, F.; Frombach, J.; Vogt, A.; Blume-Peytavi, U.; Schrade, P.; Bachmann, S.; Haag, R.; Hedtrich, S.; Schäfer-Korting, M.; Kosugi, N.; Rühl, E. Core-multishell nanocarriers: Transport and release of dexamethasone probed by soft X-ray spectromicroscopy. *J. Controlled Release* **2016**, *242*, 64−70.
(27) Brooks, J.; Everett, J.; Lermyte, F.; Tjhin, V. T.; Banerjee, S.; O'Connor, P. B.; Morris, C. M.; Sadler, P. J.; Telling, N. D.; Collingwood, J. F. Label-Free Nanoimaging of Neuromelanin in the Brain by Soft X-ray Spectromicroscopy. *Angew. Chem., Int. Ed.* **2020**, *59*, 11984−11991.
(28) Schulz, R.; Yamamoto, K.; Klossek, A.; Flesch, R.; Hönzke, S.; Rancan, F.; Vogt, A.; Blume-Peytavi, U.; Hedtrich, S.; Schäfer-Korting, M.; Rühl, E.; Netz, R. R. Data-based modeling of drug penetration relates human skin barrier function to the interplay of diffusivity and free-energy profiles. *Proc. Natl. Acad. Sci. U.S.A.* **2017**, *114*, 3631−3636.
(29) Freudiger, C. W.; Min, W.; Saar, B. G.; Lu, S.; Holtom, G. R.; He, C.; Tsai, J. C.; Kang, J. X.; Xie, X. S. Label-Free Biomedical Imaging with High Sensitivity by Stimulated Raman Scattering Microscopy. *Science* **2008**, *322*, 1857−1861.
(30) Klossek, A.; Thierbach, S.; Rancan, F.; Vogt, A.; Blume-Peytavi, U.; Rühl, E. Studies for improved understanding of lipid distributions in human skin by combining stimulated and spontaneous Raman microscopy. *Eur. J. Pharm. Biopharm.* **2017**, *116*, 76−84.
(31) Osorio-Blanco, E. R.; Rancan, F.; Klossek, A.; Nissen, J. H.; Hoffmann, L.; Bergueiro, J.; Riedel, S.; Vogt, A.; Rühl, E.; Calderón, M. Polyglycerol-Based Thermoresponsive Nanocapsules Induce Skin Hydration and Serve as a Skin Penetration Enhancer. *ACS Appl. Mater. Interfaces* **2020**, *12*, 30136−30144.
(32) Dazzi, A.; Prater, C. B.; Hu, Q.; Chase, D. B.; Rabolt, J. F.; Marcott, C. AFM-IR: Combining Atomic Force Microscopy and Infrared Spectroscopy for Nanoscale Chemical Characterization. *Appl. Spectrosc.* **2012**, *66*, 1365−1384.
(33) Kästner, B.; Johnson, C. M.; Hermann, P.; Kruskopf, M.; Pierz, K.; Hoehl, A.; Hornemann, A.; Ulrich, G.; Fehmel, J.; Patoka, P.; Rühl, E.; Ulm, G. Infrared Nanospectroscopy of Phospholipid and Surfactin Monolayer Domains. *ACS Omega* **2018**, *3*, 4141−4147.
(34) Sjövall, P.; Greve, T. M.; Clausen, S. K.; Moller, K.; Eirefelt, S.; Johansson, B.; Nielsen, K. T. Imaging of Distribution of Topically Applied Drug Molecules in Mouse Skin by Combination of Time-of-Flight Secondary Ion Mass Spectrometry and Scanning Electron Microscopy. *Anal. Chem.* **2014**, *86*, 3443−3452.
(35) DrugBank. Rapamycin DrugBank. https://www.drugbank.ca/indications/DBCOND0086651 (accessed 30 Dec 2020).
(36) Elias, P. M. Epidermal lipids, barrier function, and desquamation. *J. Invest. Dermatol.* **1983**, *80*, S44−S49.
(37) Elias, P. M. Epidermal barrier function: intercellular lamellar lipid structures, origin, composition and metabolism. *J. Controlled Release* **1991**, *15*, 199−208.
(38) Frombach, J.; Lohan, S. B.; Lemm, D.; Gruner, P.; Hasler, J.; Ahlberg, S.; Blume-Peytavi, U.; Unbehauen, M.; Haag, R.; Meinke, M. C.; Vogt, A. Protease-mediated Inflammation: An In Vitro Human Keratinocyte-based Screening Tool for Anti-inflammatory Drug Nanocarrier Systems. *Z. Phys. Chem.* **2018**, *232*, 919−933.
(39) Frombach, J.; Rancan, F.; Kübrich, K.; Schumacher, F.; Unbehauen, M.; Blume-Peytavi, U.; Haag, R.; Kleuser, B.; Sabat, R.; Wolk, K.; Vogt, A. Serine Protease-Mediated Cutaneous Inflammation: Characterization of an Ex Vivo Skin Model for the Assessment of Dexamethasone-Loaded Core Multishell-Nanocarriers. *Pharmaceutics* **2020**, *12*, 862.
(40) Suzuki, Y.; Nomura, J.; Koyama, J.; Horii, I. The role of proteases in stratum corneum: involvement in stratum corneum desquamation. *Arch. Dermatol. Res.* **1994**, *286*, 249−253.
(41) Suzuki, Y.; Nomura, J.; Hori, J.; Koyama, J.; Takahashi, M.; Horii, I. Detection and characterization of endogenous protease associated with desquamation of stratum corneum. *Arch. Dermatol. Res.* **1993**, *285*, 372−377.
(42) Leyvraz, C.; Charles, R.-P.; Rubera, I.; Guitard, M.; Rotman, S.; Breiden, B.; Sandhoff, K.; Hummler, E. The epidermal barrier function is dependent on the serine protease CAP1/Prss8. *J. Cell Biol.* **2005**, *170*, 487−496.
(43) van Smeden, J.; Janssens, M.; Boiten, W. A.; van Drongelen, V.; Furio, L.; Vreeken, R. J.; Hovnanian, A.; Bouwstra, J. A. Intercellular Skin Barrier Lipid Composition and Organization in Netherton Syndrome Patients. *J. Invest. Dermatol.* **2014**, *134*, 1238−1245.
(44) van Smeden, J.; Al-Khakany, H.; Wang, Y.; Visscher, D.; Stephens, N.; Absalah, S.; Overkleeft, H. S.; Aerts, J. M. F. G.; Hovnanian, A.; Bouwstra, J. A. Skin barrier lipid enzyme activity in Netherton patients is associated with protease activity and ceramide abnormalities. *J. Lipid Res.* **2020**, *61*, 859−869.
(45) Schulz, R.; Yamamoto, K.; Klossek, A.; Rancan, F.; Vogt, A.; Schütte, C.; Rühl, E.; Netz, R. R. Modeling of Drug Diffusion Based on Concentration Profiles in Healthy and Damaged Human Skin. *Biophys. J.* **2019**, *117*, 998−1008.
(46) Wanjiku, B.; Yamamoto, K.; Klossek, A.; Schumacher, F.; Pischon, H.; Mundhenk, L.; Rancan, F.; Judd, M. M.; Ahmed, M.; Zoschke, C.; Kleuser, B.; Rühl, E.; Schäfer-Korting, M. Qualifying X-ray and Stimulated Raman Spectromicroscopy for Mapping Cutaneous Drug Penetration. *Anal. Chem.* **2019**, *91*, 7208−7214.
(47) Yamamoto, K.; Klossek, A.; Fuchs, K.; Watts, B.; Raabe, J.; Flesch, R.; Rancan, F.; Pischon, H.; Radbruch, M.; Gruber, A. D.; Mundhenk, L.; Vogt, A.; Blume-Peytavi, U.; Schrade, P.; Bachmann, S.; Gurny, R.; Rühl, E. Soft X-ray microscopy for probing of topical tacrolimus delivery via micelles. *Eur. J. Pharm. Biopharm.* **2019**, *139*, 68−75.
(48) Ohigashi, T.; Arai, H.; Araki, T.; Kondo, N.; Shigemasa, E.; Ito, A.; Kosugi, N.; Katoh, M. Construction of the Scanning Transmission X-ray Microscope Beamline at UVSOR. *J. Phys.: Conf. Ser.* **2013**, *463*, 012006.
(49) Hitchcock, A. P.; Mancini, D. C. Bibliography and database of inner shell excitation spectra of gas phase atoms and molecules. *J. Electron Spectrosc. Relat. Phenom.* **1994**, *67*, 1−12.
(50) Hitchcock, A. P. *aXis2000 Is Written in Interactive Data Language (IDL)*. http://unicorn.mcmaster.ca/aXis2000.html, 25.07.2017; McMaster University, 1997.
(51) Henke, B. L.; Gullikson, E. M.; Davis, J. C. X-ray Interactions: Photoabsorption, Scattering, Transmission, and Reflection at E = 50−30,000 eV, Z = 1−92. *At. Data Nucl. Data Tables* **1993**, *54*, 181−342.
(52) Koprinarov, I. N.; Hitchcock, A. P.; McCrory, C. T.; Childs, R. F. Quantitative mapping of structured polymeric systems using singular value decomposition analysis of soft X-ray images. *J. Phys. Chem. B* **2002**, *106*, 5358−5364.
(53) Lerotic, M.; Mak, R.; Wirick, S.; Meirer, F.; Jacobsen, C. MANTiS: a program for the analysis of X-ray spectromicroscopy data. *J. Synchrotron Radiat.* **2014**, *21*, 1206−1212.
(54) Stöhr, J. *NEXAFS Spectroscopy*; Springer: Berlin, 1992.

(55) Akiyama, M. Corneocyte lipid envelope (CLE), the key structure for skin barrier function and ichthyosis pathogenesis. *J. Dermatol. Sci.* **2017**, *88*, 3−9.
(56) Lazo, N. D.; Meine, J. G.; Downing, D. T. Lipids Are Covalently Attached to Rigid Corneocyte Protein Envelopes Existing Predominantly as β-Sheets: A Solid-State Nuclear Magnetic Resonance Study. *J. Invest. Dermatol.* **1995**, *105*, 296−300.
(57) Le Lamer, M.; Pellerin, L.; Reynier, M.; Cau, L.; Pendaries, V.; Leprince, C.; Méchin, M.-C.; Serre, G.; Paul, C.; Simon, M. Defects of corneocyte structural proteins and epidermal barrier in atopic dermatitis. *Biol. Chem.* **2015**, *396*, 1163−1179.
(58) Kirschner, N.; Brandner, J. M. Barriers and more: functions of tight junction proteins in the skin. *Ann. N.Y. Acad. Sci.* **2012**, *1257*, 158−166.
(59) Isacke, C. M.; Horton, M. A. Occludin. In *The Adhesion Molecule FactsBook*, 2nd ed.; Isacke, C. M., Horton, M. A., Eds.; Academic Press: London, 2000; pp 300−301.
(60) Sun, L.; Liu, Z.; Lin, Z.; Cun, D.; Tong, H.; Yan, R.; Wang, R.; Zheng, Y. Comparison of normal versus imiquimod-induced psoriatic skin in mice for penetration of drugs and nanoparticles. *Int. J. Nanomed.* **2018**, *13*, 5625−5635.
(61) Radbruch, M.; Pischon, H.; Ostrowski, A.; Volz, P.; Brodwolf, R.; Neumann, F.; Unbehauen, M.; Kleuser, B.; Haag, R.; Ma, N.; Alexiev, U.; Mundhenk, L.; Gruber, A. D. Dendritic Core-Multishell Nanocarriers in Murine Models of Healthy and Atopic Skin. *Nanoscale Res. Lett.* **2017**, *12*, 64.
(62) Iwai, I.; Han, H.; den Hollander, L.; Svensson, S.; Öfverstedt, L.-G.; Anwar, J.; Brewer, J.; Bloksgaard, M.; Laloeuf, A.; Nosek, D.; Masich, S.; Bagatolli, L. A.; Skoglund, U.; Norlén, L. The Human Skin Barrier Is Organized as Stacked Bilayers of Fully Extended Ceramides with Cholesterol Molecules Associated with the Ceramide Sphingoid Moiety. *J. Invest. Dermatol.* **2012**, *132*, 2215−2225.

https://doi.org/10.1021/acsomega.1c01058
ACS Omega 2021, 6, 12213−12222